DOI: 10.7589/2019-09-231

Journal of Wildlife Diseases, 56(4), 2020, pp. 759–767

COUNTCOLORS, AN R PACKAGE FOR QUANTIFICATION OF THE FLUORESCENCE EMITTED BY *PSEUDOGYMNOASCUS DESTRUCTANS* LESIONS ON THE WING MEMBRANES OF HIBERNATING BATS

Sarah E. Hooper,[1,4,5,6] Hannah Weller,[2,5] and Sybill K. Amelon[3,5]

[1] Department of Veterinary Pathobiology, College of Veterinary Medicine, University of Missouri, 202 Anheuser-Busch Natural Resource Building, Columbia, Missouri 65211, USA
[2] Department of Ecology and Evolutionary Biology, Brown University Biomedical Center, 171 Meeting Street, Providence, Rhode Island 02912, USA
[3] US Department of Agriculture, US Forest Service Northern Research Station, 202 Anheuser-Busch Natural Resource Building, Columbia, Missouri 65211, USA
[4] Department of Biomedical Sciences, Ross University School of Veterinary Medicine, PO Box 334, Basseterre, St. Kitts, West Indies
[5] These authors contributed equally to this study.
[6] Corresponding author (email: sarahdvm.ugamizzou@gmail.com)

ABSTRACT: *Pseudogymnoascus destructans* colonizes the wing membrane of hibernating bats with the potential to form dense fungal hyphae aggregates within cupping erosions. These fungal cupping erosions emit a characteristic fluorescent orange-yellow color when the wing membrane is transilluminated with 385 nm ultraviolet (UV) light. The purpose of this study was to create and validate the R package, countcolors, for quantifying the distinct orange–yellow UV fluorescence in bat-wing membrane lesions caused by *P. destructans*. Validation of countcolors was completed by first quantifying the percent area of 20, 2.5 cm^2 images. These generated images were of two known pixel colors ranging from 0% to 100% of the pixels. The countcolors package accurately measured the known proportion of a given color in each image. Next, 40, 2.5 cm^2 sections of UV transilluminated photographs of little brown bat (*Myotis lucifugus*) wings were given to a single evaluator. The area of fluorescence was both manually measured and calculated using image analysis software and quantified with countcolors. There was good agreement between the two methods (Pearson's correlation=0.915); however, the manual use of imaging software showed a consistent negative bias. Reproducibility of the analysis methods was tested by providing the same images to naive evaluators who previously never used the software; no significant difference (P=0.099) was found among evaluators. Using the R package countcolors takes less time than does manually measuring the fluorescence in image analysis software, and our results showed that countcolors can improve the accuracy when quantifying the area of *P. destructans* infection in bat wing-membranes.

Key words: Bat, color quantification, fungal infection, *Myotis lucifugus*, *Pseudogymnoascus destructans*, R package, UV transillumination photographs, white-nose syndrome.

INTRODUCTION

Pseudogymnoascus destructans is the causative agent of white-nose syndrome (WNS), a disease that has caused severe population declines in eastern North American hibernating bat species (Frick et al. 2010; Turner et al. 2011; O'Shea et al. 2016) and has caused regional extirpation of some species such as the northern long-eared bat (*Myotis septentrionalis*; Colatskie 2017). During hibernation, *P. destructans* colonizes the epidermal surface of bats. This colonization can lead to dense fungal hyphal aggregates invading the epidermis and dermis, resulting in cup-like intraepidermal colonies, or cupping erosions (Meteyer et al. 2009). The fungal cupping lesions emit a characteristic orange-yellow fluorescence color when the wing membrane is transilluminated with 360 nm ultraviolet (UV) light (Turner et al. 2014). The UV transillumination method of identifying WNS lesions has been shown to correlate well with histological assessment, the gold standard for identifying *P. destructans* lesions over 20–40 μm in diameter, with smaller lesions requiring digital computer magnification of the images (Turner et al. 2014). Many studies have

captured digital images of UV transilluminated bat wings to noninvasively assess the extent of *P. destructans* cupping erosions as well as determining a quantitative PCR (qPCR; fungal load) and histological analysis (McGuire et al. 2016; Zukal et al. 2016; Pikula et al. 2017; Bandouchova et al. 2018).

Capturing UV light photographs of bat wings is easily achieved by researchers and conservation management agency personnel; however, analyzing the images is difficult due to the time-consuming nature of the available methods. Two main methods are used when manually quantifying the *P. destructans* cupping erosions in UV photographs. The first requires manually outlining every UV fluorescing area using proprietary or open-source software (McGuire et al. 2016). The second requires manual counting of lesions using image analysis software (Zukal et al. 2016). However, this method ignores the size and shape of the lesions. The reliance upon manual methods is a bottleneck for many WNS studies and has caused many researchers and wildlife agencies to underutilize UV transillumination photographs to track the disease progression of WNS.

Digital images are typically displayed as a series of pixels on an X-Y grid, and the color of each pixel is expressed using the red-green-blue (RGB) color space. All colors in RGB color space are expressed as a combination of red, green, and blue brightness values, each of which varies between 0 (no brightness) and 255 (maximum brightness). For example, a black pixel would have an RGB value of (0, 0, 0), whereas a pure red pixel would have an RGB value of (255, 0, 0). The distinct orange-yellow fluorescence color emitted by *P. destructans* lesions takes on a set range of RGB color values in digitally captured UV transilluminated bat wing images. The locations of these orange-yellow pixels can therefore be tracked by providing this expected color range. Using R, a free software environment for statistical computing and graphics (R Core Team 2017), we created the R package, countcolors.

Our R package allows users to count the number of pixels that comprise the orange-yellow fluorescence of the lesions caused by *P. destructans*, based upon the RGB colors caused by infection as defined by the user, thereby allowing semiautomated quantification of the fluorescing infection from transilluminated photographs of bat wings. We report the development and validation of the countcolors package and its use to test our hypothesis that countcolors would yield the same percent area of fluorescing cupping lesions caused by *P. destructans* within the wing membranes as would manually identifying the fluorescing area to determine the percent area of *P. destructans* lesions.

MATERIALS AND METHODS

All activities conducted in this study were conducted under an approved University of Missouri Institutional Animal Care and Use Committee protocol and Missouri Department of Conservation Wildlife Scientific Collection permits (15556 and 16409). Disinfection protocols for bat studies (US Fish and Wildlife Service 2016) were followed for collection and sampling activities.

Creation and validation of R-package

Countcolors counts pixels using a user-defined RGB color range or ranges. The output includes the locations of the pixels in the images, a masked version of the image with targeted pixels changed to a color specified by the user, and the percentage of pixels that compose the image that are within the user-defined color range. Optional background masking can be used to ignore a single color or multiple color ranges. The released version of countcolors is available online (Weller 2019) as is the development version and the installation instructions (Weller 2018). To validate the countcolors package, we created 20, 1,000 pixel^2 images (2.54×2.54 cm). Each image consisted of two RGB colors, with the specific number of pixels known for each RGB color. The generated images ranged from 0% to 100% in 5% increments.

Transillumination photographs

Collecting and photographing hibernating adult little brown bats (*Myotis lucifugus*) are described in Amelon et al. (2017). Briefly, hibernating adult little brown bats were collected from privately owned hibernacula with the landowner's permission and transferred to an artificial hibernaculum

as part of a study assessing compounds reported to inhibit the growth of *P. destructans*. Each bat had UV transillumination photographs (360–385 nm) taken following Turner et al. (2014). Photographs were taken with a digital SLR camera (Canon E0S Rebel XT, Canon USA, Inc., Melville, New York, USA) with a standard zoom lens (Canon EF-S 18-55 mm f/3.5-5.6 IS) mounted on a tripod. Based upon a one-way analysis of variance (ANOVA) and correlation bivariate normal model a priori power analysis performed in G*Power (Faul et al. 2009), photographs from a subset of animals (n=40) were used for this study.

Image preparation and manual measurements of the WNS fluorescence lesions

Similar to the validation procedure, 2.54 cm^2 images were created using the UV images of *P. destructans*-infected bat wings. The polygonal lasso tool in Adobe Photoshop CC 2018 (Adobe Systems, San Jose, California, USA) was used to select the predefined 2.54 cm^2 area of each wing and copy it to a new layer. The new layer was saved as a JPEG file which consisted of the selected wing membrane square and a white background. To manually measure and calculate the percent area of fluorescent cupping lesions in the 40 predefined, 2.54 cm^2 wing-membrane images, we combined the methods previously described by McGuire et al. (2016) and Zukal et al. (2016). Using the polygon selections tool, each orange-yellow fluorescing lesion was outlined and the area in pixels saved using the measurements function in ImageJ (version 1.52a; Schneider et al. 2012). The entire image was measured in pixels and the total surface area was calculated. The wing surface affected by the fluorescing lesions was calculated and the percentage of wing surface affected determined by calculation.

Measurement of WNS fluorescing lesions using countcolors

Countcolors was used to measure and calculate the area of *P. destructans* fluorescent lesions in the identical 40 predefined, 2.54 cm^2 wing-membrane images used for the manual measurement process. An explanatory vignette with illustrated, detailed step-by-step directions on calculating the percentage of *P. destructans* fluorescent lesions is available online (Hooper 2019). Briefly, lines preceded by ">" indicate commands executed in the R console within Rstudio 1.1.383 (R Studio Team 2016). For this study, the R package jpeg (Urbanek 2014) and the developmental version of the R package countcolors were downloaded, loaded into R-Studio, and the working directory set to a folder designated for this project.

```
> library(countcolors)
> library(jpeg)
> setwd("[path/to/directory]/Name_of_designated_folder")
```

Vectors were created for the upper bounds (upperbackground) and lower bounds (lowerbackground) of the white background pixels in standard RGB format.

```
> upperbackground <- c(1, 1, 1)
> lowerbackground <- c(0.8, 0.8, 0.8)
```

Vectors were created for the color range of the orange-yellow fluorescence for each photograph by defining the lower and upper limit for each of the three color channels in standard RGB format.

```
> lower.rectangular <-c(red_value, green_value, blue_value)
> upper.rectangular <-c(Red value, green_value, blue_value)
```

Countcolors can be used either to count only the pixels in the defined color range or to count the pixels in the defined color range and a specific radius surrounding the pixel. The rectangular color range was selected to only count the pixels in the defined color range of the orange-yellow fluorescence pixels. Each photograph was plotted, and the target color range was replaced by a solid magenta color.

```
> wingimage <- countcolors::countcolors("[path/to/directory]/Name_of_image_for_analysis"), color.range = "rectangular", upper = upper.rectangular, lower = lower.rectangular, bg.upper=upperbackground, bg.lower =lowerbackground, target.color = "magenta", plot= TRUE)
```

Each plotted image was saved as a scalable vector graphics file. The saved scalable vector graphics file was opened in Adobe Photoshop with 236 pixels/cm resolution and checked by magnifying the images up to 1,000% to ensure that only the orange-yellow fluorescence was replaced by the magenta color (Fig. 1). The defined color range for the orange-yellow fluorescence was altered only if additional orange-yellow fluorescence was observed or areas of non–orange-yellow fluorescence were replaced by the magenta target color. After ensuring all the areas of *P. destructans* infection were replaced by the magenta target color, the percentage of the wing where *P. destructans* lesions had formed was determined.

```
> wingimage$pixel.fraction
```

Assessment of method reproducibility

To assess the reproducibility of both methods, we recruited two observers with no prior experience with UV-transilluminated wing images, the analysis methods, or the analysis programs. The observers were provided with approximately 1 h of instruction on how to use the analysis software and how to perform the two described analysis methods. Then the observers were provided the

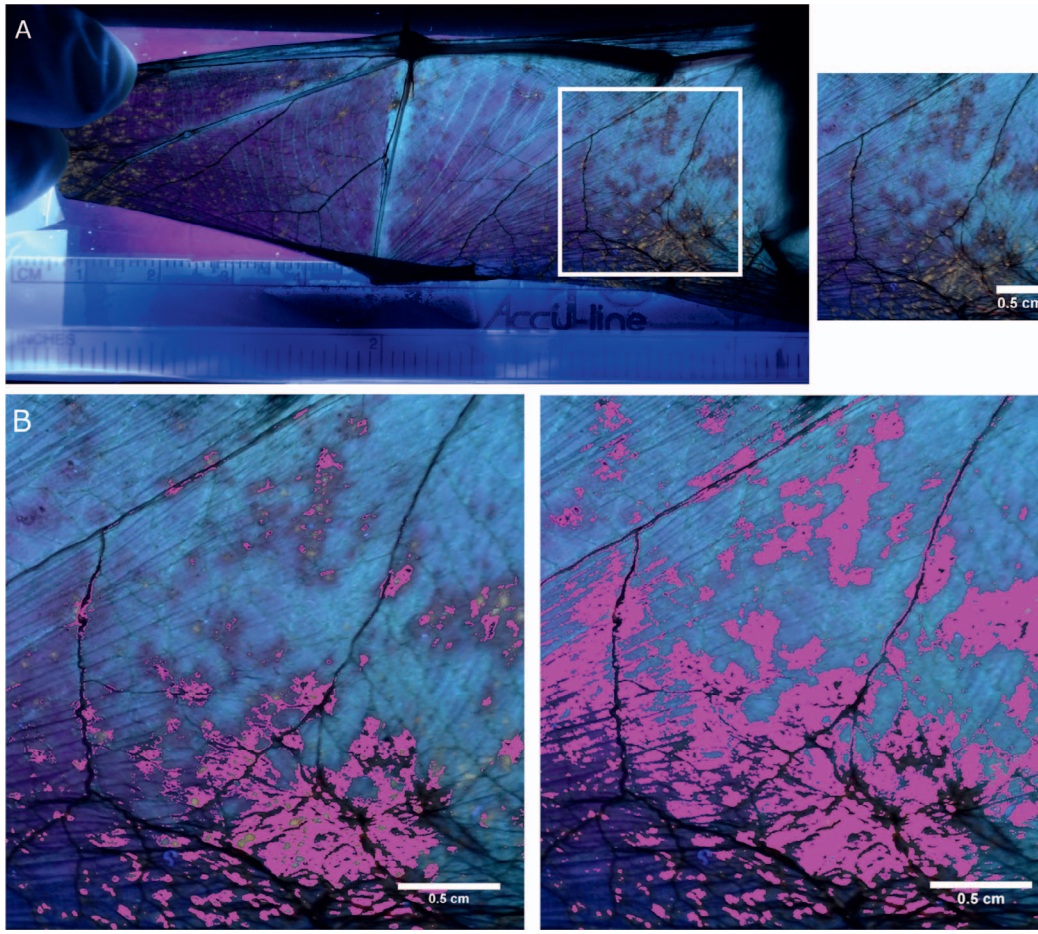

FIGURE 1. R package countcolors was used to determine the percent area of orange-yellow fluorescence caused by cutaneous *Pseudogymnoascus destructans* lesions in a little brown bat (*Myotis lucifugus*) wing section. (A) The right wing of a little brown bat transilluminated by 385 nm ultraviolet light with a 2.54 cm^2 section of wing outlined in white. Both countcolors and manual identification of the *P. destructans* lesions were quantified in a 2.54 cm^2 section of each wing to ensure all images were a standard size. (B) Countcolors generates a masked version of the original image by changing the user-defined target pixel colors to a specified color. This masked image allows visual confirmation that the user-defined color range identified all orange-yellow fluorescence. If the magenta color did not replace all orange-yellow fluorescence indicating cutaneous *P. destructans* lesions (left image) or replaced normal wing tissue, then the color range was redefined to ensure all the fluoresce from the lesions were replaced by magenta color (right image).

same 2.54 cm^2 wing-membrane images that were analyzed by the initial evaluator.

Statistical analyses

All statistical analyses were performed using R 3.4.2 (R Core Team 2017). Normality of the percent area of lesion fluorescence was assessed using the Shapiro-Wilk test. We normalized the data using a square root transformation. The R package mcr version 1.2.1 (Manuilova et al. 2014) was used to perform Deming regression and calculate the Pearsons product-moment correlation coefficient to determine overall agreement, alternatively phrased as the estimate of the degree of association, of the percentage of *P. destructans* lesion fluorescence between the two methods. A bias plot was constructed in accordance with Bland and Altman (1986) by plotting the mean percentage of *P. destructans* lesion fluorescence obtained by using the two methods on the x-axis and plotting the difference between their mean values on the y-axis using the R package blandr (Datta 2017). Additionally, the mean percentage

of the wing infected by *P. destructans* from both methods was compared with a one-way ANOVA. Interrater reliability was assessed by calculating the intraclass correlation coefficient (ICC) using a two-way model random effects model and consistency as the defined relationship type for each method using R package irr version 0.84.1 (Gamer et al. 2019). A two-way ANOVA was conducted to compare the percentage of the wing infected by *P. destructans* measured by all observers from both methods.

RESULTS

Validation of countcolors

Creating two-tone 1,000 pixel^2 images ranging from 0% to 100% of two defined RGB colors resulted in a 2 pixel-wide gradient between the two colors; therefore, a color range was required to be defined. Implementation of the color range resulted in the countcolors results having a correlation coefficient of 1.

Manual ImageJ measurements vs countcolors

Forty UV-transilluminated photographs were selected to determine if the semiautomation quantification of *P. destructans* lesion fluorescence with countcolors would yield the same percent area of fluorescent lesions as manual calculations. Ten attempts were required to establish the initial defined color range. The upper pixel RGB ranges were held constant for all images, whereas the lower pixel RGB ranges were altered four times. The alteration of the color range was primarily based upon the date of the photograph. The orange-yellow fluorescence color emitted by *P. destructans* epidermal erosions ranged from less than 1% to 43.6% of the predefined wing surface area as determined by manual calculations. The range increased using the countcolors package, with the orange-yellow fluorescence epidermal erosions ranging from less than 1% to 81.4% of the predefined wing surface area. The mean percentage of the wing covered by *P. destrucans* fluorescent lesions did not statistically differ between the two methods (F=2.124, P=0.149). Regression analysis revealed that the two methods showed good agreement (Fig. 2; Pearson's correlation=0.915). The slopes of the regression lines (Fig. 2) and analysis of the Bland-Altman plot (Fig. 3) revealed that as the colonization of *P. destructans* on the wing membrane increased, the manual calculations consistently underestimated the surface area of the fungal infection.

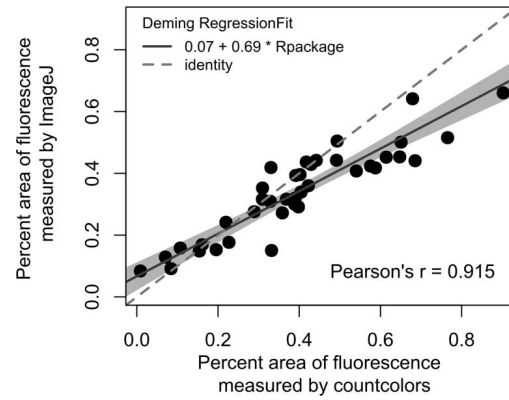

FIGURE 2. Comparison of ImageJ (version 1.52a; Schneider et al. 2012) and countcolor R package in calculating the percent area fluorescence caused by *Pseudogymnoascus destructans* in the same little brown bat (*Myotis lucifugus*) wing section shown. Deming regression, which accounts for potential errors in measurements obtained by ImageJ and countcolors methods, was used to determine that the area of fluorescence determined by ImageJ (y-axis) and the area of fluorescence determined by countcolors (x-axis) showed good agreement (Pearson's correlation=0.915). Each point represents the measurement of area fluorescence by ImageJ and countcolors for the same image and the line of best fit is shown as a solid black line. The 95% confidence intervals are shown in gray. The identity line (dashed) shows when the two methods obtain equal measurements for the area of fluorescence.

Method reproducibility

The interrater reliability for the manual method was moderate with an ICC of 0.74 and was good for countcolors with an ICC of 0.78. The mean percentage of the wing covered by fluorescing *P. destructans* lesions did not statistically differ among the three observers (F=2.753, P=0.0993).

DISCUSSION

The use of UV transillumination of the wing membranes of hibernating bats has the

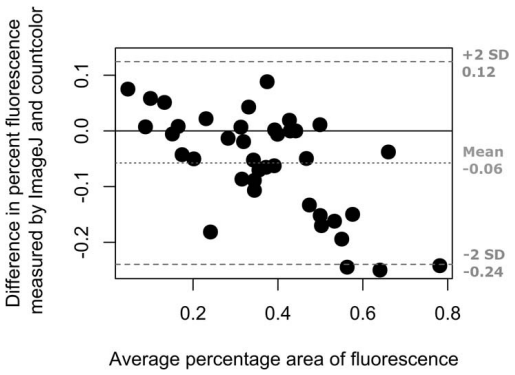

FIGURE 3. Bland-Altman plot showing the quantitative agreement between councolors and ImageJ in calculating the percent area of fluorescence caused by *Pseudogymnoascus destructans* in the same little brown bat (*Myotis lucifugus*) wing section. Each point represents the measurement of the percent area fluorescence by ImageJ and countcolors for the same image. The solid black horizontal line shows the exact agreement, a bias of 0, and the dotted horizontal gray line indicates the mean of the difference between the results for the two analysis methods. The gray dashed lines indicate two SDs, or the boundaries of the 95% confidence interval.

potential to be a powerful, noninvasive, and nonlethal sampling technique for tracking disease progression at hibernacula by assessing the intensity of *P. destructans* fluorescent lesions and for tracking disease progression of individuals (Turner et al. 2014). Utilization of this research and management tool should be employed only during fall swarming, spring emergence, summer, and, if deemed necessary, as close to the end of hibernation as possible. Using this technique repeatably throughout hibernation will decrease survival due to the consumption of fat stores caused by repeated arousals and the stress from handling.

The UV transillumination technique has been employed in a number of studies in order to collect biopsy samples (Lučan et al. 2016; Zukal et al. 2016; Pikula et al. 2017), to confirm the presence or absence of fluorescing fungal metabolites presumed to result from *P. destructans* infection (Mascuch et al. 2015), or in conjunction with qPCR results (Bernard and McCracken 2017). Few studies have used the transillumination technique as a measure of cutaneous invasive ascomycosis of the wing-membrane because the manual analysis of the photographs is labor-intensive and time-consuming. Countcolors was designed to allow semiautomation of the analysis of UV transillumination photographs of bats whose wing membrane is infected by *P. destructans*, thereby reducing the time and labor required for image analysis.

The few studies that have reported measuring disease severity based upon the fluorescence of *P. destructans* lesions have reported the results as number of fluorescent lesions per wing (Lučan et al. 2016; Bandouchova et al. 2018) or the percentage of fluorescent area on the wing membrane (McGuire et al. 2016; Moore et al. 2018). We designed countcolors to report the pixel number and percent of the image, in this case a bat wing, covered by the defined pixel range. Reporting the percentage of the wing emitting the orange-yellow fluorescence allows a repeatable, quantitative analysis that is not affected by minor changes in the focal length of the photographic lens used. Additionally, reporting on a percent area of the wing-membrane accounts for the size variation observed in *P. destructans* fluorescing lesions (Figs. 1, 2) and enhances the ability for a quantitative, nonbiased comparison between species with different wing surface areas.

Studies reporting UV transillumination results based upon the percentage of fluorescent area on the wing membrane have relied upon two computational software programs, Photoshop and ImageJ (Schneider et al. 2012; McGuire et al. 2016; Cheng et al. 2017). Cheng et al. (2017) was the first study to describe using Photoshop for quantification of UV fluorescence. One disadvantage of the Cheng et al. (2017) method is having to first manipulate the color and brightness of the images prior to analysis. Once the image was altered, the method required a series of steps to obtain a histogram of similarly colored orange pixels, which could then be manually counted and used to calculate the percent of fluorescence of the wing (Cheng et al. 2017). Countcolors does not require color and brightness manipulation prior to analysis; rather, the

user is able to alter the defined color range as required. Additionally, countcolors allows selection of the exact pixel colors from a location anywhere within the image file. When Photoshop is used, only a single pixel color is initially selected and selected similar pixel colors are required to be touching the initial color pixel. Our initial attempts to replicate this method resulted in the lesions being incompletely selected or selection of portions of the wing that were not covered by *P. destructions* cupping erosions. Cheng et al. (2017) analyzed inoculated little brown bats with a smaller reported range of *P. destructans* intradermal lesions which were likely more uniform, whereas our photographs were from naturally infected little brown bats. It is possible that Photoshop was unable to correctly select the fluorescence lesions from naturally infected little brown bats because of the large range of *P. destructans* intradermal colonization, nonuniform lesions, and various colors of wing pigmentation around the lesions.

The commonly utilized image software is ImageJ, an opensource software available in the public domain (Schneider et al. 2012). Observers using ImageJ are required to manually trace each fluorescent lesion to calculate the area of fluorescence (McGuire et al. 2016). ImageJ plugins are too limited in the number of colors they can count (Pichette 2010) or they rely on measuring objects in binary or threshold images (Ferreira and Rasband 2012), which are unable to distinguish pinpoint fluorescence of *P. destructans* lesions from nonfluorescing areas. Manually hand tracing each lesion is time-consuming with each image used in our study requiring 30–360 min to analyze, which makes routine analysis unfeasible for both researchers and management agencies desiring to track disease progression within individuals and hibernacula. Using countcolors, batch analysis of images can be completed within seconds to hours depending on the number of files, size of the files, and processing speed of the computer. Additionally, our study supports the observation that enlisting multiple workers to hand trace each lesion results in less consistent or unreproducible results because there was only moderate interrater agreement between multiple observers when assessed by ICC; however, the interrater agreement increased to good agreement when using councolors. By using countcolors, the observer can avoid underestimating the fungal lesions, because each image can be checked to ensure that all the *P. destructans*-induced orange-yellow fluorescence is replaced by a single solid color.

It is essential that each masked image be checked to ensure the user-defined color range selects all fluorescent pixels, because the cutaneous invasive *P. destructans* lesions fluoresce due to the accumulation of riboflavin (Flieger et al. 2016). The fluorescent color emitted by riboflavin can be altered based upon controllable variables, such as the wavelength of light used to backlight the wing membrane, and noncontrollable environmental variables such as the temperature of the environment (Weber 1950). In our experience, the lower limit of the defined RGB colors for a set of UV-transilluminated wing photographs taken in a controlled research setting was 0.28235 (red), 0.34902 (blue), and 0.45882 (green). For a set of UV-transilluminated wing photographs acquired in the field during the end of hibernation, the upper limit of the defined RGB colors was 0.6667 (red), 0.59608 (blue), and 0.58824 (green). Additionally, the camera settings will affect the color captured in digital photographs; therefore, a universal defined color range cannot exist. If a universal defined color range were to be used, it could result in the under- or overreporting of the *P. destructans*-fluorescing lesions.

Additionally, countcolors has the potential to increase the sensitivity of UV-transillumination. McGuire et al. (2016) reported that UV fluorescence was less sensitive than was qPCR and histology. Using countcolors, defined orange-yellow florescence target color ranges can be used to search photographs and allow the user to determine if digital magnification is required to visualize the fluorescent lesions, because lesions under 20 μm are visible only with magnification (Turner et al. 2014).

In summary, our study validated that countcolors is able to repeatably and objectively quantify the color range defined by the user. Furthermore, we demonstrated that countcolor can be used effectively to semi-automate the analysis of fluorescence emitted from *P. destructans* lesions from UV transilluminated photographs of bat wings.

ACKNOWLEDGMENTS

This project was supported financially by US Department of Agriculture, US Forest Service (16-JV-11242311-118), Missouri Department of Conservation (CA 416), and US Fish and Wildlife Service (17-AI11242311006). We thank Shannon Ehlers and Jeanne Mihail for reviewing this manuscript prior to submission.

LITERATURE CITED

Amelon SK, Hooper SE, Womack KM. 2017. Bat wing biometrics: Using collagen-elastin bundles in bat wings as a unique individual identifier. *J Mammal* 98: 744–751.

Bandouchova H, Bartonička T, Berkova H, Brichta J, Kokurewicz T, Kovacova V, Linhart P, Piacek V, Pikula J, Zahradníková A, et al. 2018. Alterations in the health of hibernating bats under pathogen pressure. *Sci Rep* 8:6067.

Bernard RF, McCracken GF. 2017. Winter behavior of bats and the progression of white-nose syndrome in the southeastern United States. *Ecol Evol* 7:1487–1496.

Bland JM, Altman DG. 1986. Statistical methods for assessing agreement between two methods of clinical measurement. *Lancet* 1:307–310.

Cheng TL, Mayberry H, McGuire LP, Hoyt JR, Langwig KE, Nguyen H, Parise KL, Foster JT, Willis CKR, Kilpatrick AM, et al. 2017. Efficacy of a probiotic bacterium to treat bats affected by the disease white-nose syndrome. *J Appl Ecol* 54:701–708.

Colatskie S. 2017. Missouri bat hibernacula survey results from 2011–2017, following white-nose syndrome arrival. *Missouri Department of Conservation Technical Brief*. Missouri Department of Conservation, Jefferson City, Missouri, 14 pp.

Datta D. 2017. *Blandr: A Bland-Altman method comparison package for R*. https://github.com/deepankardatta/blandr. Accessed September 2018.

Faul F, Erdfelder E, Buchner A, Lang A-G. 2009. Statistical power analyses using G*Power 3.1: Tests for correlation and regression analyses. *Behav Res Methods* 41:1149–1160.

Ferreira T, Rasband W. 2012. *ImageJ user guide—IJ 1.46*. https://imagej.nih.gov/ij/docs/guide/user-guide.pdf. Accessed January 2016.

Flieger M, Bandouchova H, Cerny J, Chudíčková M, Kolarik M, Kovacova V, Martíinková N, Novák P, Šebesta O, Stodůlková E, et al. 2016. Vitamin B_2 as a virulence factor in *Pseudogymnoascus destructans* skin infection. *Sci Rep* 6:33200.

Frick WF, Pollock JF, Hicks AC, Langwig KE, Reynolds DS, Turner GG, Butchkoski CM, Kunz TH. 2010. An emerging disease causes regional population collapse of a common North American bat species. *Science* 329:679–682.

Gamer M, Lemon J, Fellows I, Singh P. 2019. *Irr: Various coefficients of interrater reliability and agreement*. https://CRAN.R-project.org/package=irr. Accessed September 2019.

Hooper S. 2019. *Example quantification of WNS lesions on bat wings*. https://cran.r-project.org/web/packages/countcolors/vignettes/bat_WNS.html. Accessed January 2019.

Lučan RK, Bandouchova H, Bartonička T, Pikula J, Zahradníková A, Zukal J, Martinkováa N. 2016. Ectoparasites may serve as vectors for the white-nose syndrome fungus. *Parasit Vectors* 9:16.

Manuilova E, Schuetzenmeister A, Model F. 2014. *Mcr: Method comparison regression*. https://CRAN.R-project.org/package=mcr. Accessed September 2018.

Mascuch SJ, Moree WJ, Hsu CC, Turner GG, Cheng TL, Blehert DS, Kilpatrick AM, Frick WF, Meehan MJ, Dorrestein PC, et al. 2015. Direct detection of fungal siderophores on bats with white-nose syndrome via fluorescence microscopy-guided ambient ionization mass spectrometry. *PLoS One* 10:e0119668.

McGuire LP, Turner JM, Warnecke L, McGregor G, Bollinger TK, Misra V, Foster JT, Frick WF, Kilpatrick AM, Willis CK. 2016. White-nose syndrome disease severity and a comparison of diagnostic methods. *EcoHealth* 13:60–71.

Meteyer CU, Buckles EL, Blehert DS, Hicks AC, Green DE, Shearn-Bochsler V, Thomas NJ, Gargas A, Behr MJ. 2009. Histopathologic criteria to confirm white-nose syndrome in bats. *J Vet Diagn Investig* 21:411–414.

Moore MS, Field KA, Behr MJ, Turner GG, Furze ME, Stern DWF, Allegra PR, Bouboulis SA, Musante CD, Vodzak ME, et al. 2018. Energy conserving thermoregulatory patterns and lower disease severity in a bat resistant to the impacts of white-nose syndrome. *J Comp Physiol* 188:163–176.

O'Shea TJ, Cryan PM, Hayman DTS, Plowright RK, Streicker G. 2016. Multiple mortality events in bats: A global review. *Mammal Rev* 46:175–190.

Pichette B. 2010. *Color pixel counter*. http://imagejdocu.tudor.lu/doku.php?id=plugin:color:color_pixel_counter:start. Accessed January 2016.

Pikula J, Amelon SK, Bandouchova H, Bartonička H, Berkova H, Brichta J, Hooper S, Kokurewicz T, Kolarik M, Köllner B, et al. 2017. White-nose syndrome pathology grading in nearctic and palearctic bats. *PLoS One* 12:e0180435.

R Core Team. 2017. *R: A language and environment for statistical computing*. R Foundation for Statistical

Computing, Vienna, Austria. https://www.R-project.org/. Accessed March 2018.

RStudio Team. 2016. *RStudio: Integrated development for R*. RStudio, Inc., Boston, Massachusetts. http://www.rstudio.com/. Accessed March 2018.

Schneider CA, Rasband WS, Eliceiri KW. 2012. NIH Image to ImageJ: 25 years of image analysis. *Nat Methods* 9:671–675.

Turner GG, Meteyer CU, Barton H, Gumbs JF, Reeder DM, Overton B, Bandouchova H, Bartoničcka T, Martíinkováa N, Pikula J, et al. 2014. Nonlethal screening of bat-wing skin with the use of ultraviolet fluorescence to detect lesions indicative of white-nose syndrome. *J Wildl Dis* 50:566–573.

Turner GG, Reeder DM, Coleman JTH. 2011. A five-year assessment of mortality and geographic spread of white-nose syndrome in north american bats and a look to the future. *Bat Res News* 52:13–27.

Urbanek S. 2014. *Jpeg: Read and write JPEG images. R package version 0.1-8*. https://cran.r-project.org/src/contrib/Archive/jpeg/. Accessed January 2016.

US Fish and Wildlife Service. 2016. *National white-nose syndrome decontamination protocol version 04.12.2016*. https://www.whitenosesyndrome.org/topics/decontamination. Accessed February 2016.

Weber G. 1950. Fluorescence of riboflavin and flavin-adenine dinucleotide. *Biochem J* 47:114–121.

Weller H. 2018. *Countcolors*. https://github.com/hiweller/countcolors. Accessed June 2018.

Weller H. 2019. *Countcolors: Locates and counts pixels within color range(s) in images*. https://cran.r-project.org/web/packages/countcolors/index.html. Accessed April 2019.

Zukal J, Bandouchova H, Brichta J, Cmokova A, Jaron KS, Kolarik M, Kovacova V, Kubátová A, Nováková A, Orlov O, et al. 2016. White-nose syndrome without borders: *Pseudogymnoascus destructans* infection tolerated in Europe and palearctic Asia but not in North America. *Sci Rep* 6:19829.

Submitted for publication 12 September 2019.
Accepted 30 January 2020.